J. theor. Biol. (2001) **210,** 201–219
doi:10.1006/jtbi.2000.2287, available online at http://www.idealibrary.com on IDEAL®

Non-local Concepts and Models in Biology

C. T. Lee, M. F. Hoopes, J. Diehl, W. Gilliland, G. Huxel, E. V. Leaver, K. McCann, J. Umbanhowar and A. Mogilner

Institute of Theoretical Dynamics, University of California, Davis, CA 95616, *U.S.A.*

(*Received on* 21 *October* 1998, *Accepted in revised form on* 21 *January* 2000)

In this paper, we consider local and non-local spatially explicit mathematical models for biological phenomena. We show that, when rate differences between fast and slow local dynamics are great enough, non-local models are adequate simplifications of local models. Non-local models thus avoid describing fast processes in mechanistic detail, instead describing the effects of fast processes on slower ones. As a consequence, non-local models are helpful to biologists because they describe biological systems on scales that are convenient to observation, data collection, and insight. We illustrate these arguments by comparing local and non-local models for the aggregation of hypothetical organisms, and we support theoretical ideas with concrete examples from cell biology and animal behavior.

1. Introduction

Biological interactions occur at specific locations and frequently involve the redistribution of organisms or molecules in space. Even from initially homogeneous states, striking patterns can form that make space heterogeneous (Levin & Segel, 1985; Levin, 1992; Mackas & Boyd, 1979; Steele, 1974, 1976, 1978). Recognizing the importance of space, biologists have struggled with the difficulties of collecting data over numerous spatial scales. Models can facilitate biological explorations by allowing researchers to make predictions and explore questions difficult to address with field or lab studies. Over the past seven decades, researchers have developed a variety of ways of modeling spatial interactions in biology, starting with Fisher's (1937) seminal work on gene spread. This paper examines the ways in which spatially explicit non-local models help biologists to capture essential features of spatial phenomena.

We begin our investigation by briefly describing several different approaches to modeling biological systems. Because our discussion encompasses widely different biological disciplines including ecology, genetics, physiology, and cell biology, the language of this initial summary is intentionally general. For the purposes of this paper, for instance, we consider biological systems to be collections of interacting individuals that coexist on a spatial landscape. These "individuals" can represent cells, molecules, or organisms. In order for individuals to interact, they may move across space themselves or some agent related to them may move. Keeping the possibility of related agents in mind, however, we will refer only to "interacting individuals". Meanwhile, modelers may capture individual movement by following the individuals themselves or by following their densities. For the present, we restrict our attention to models that consider density as a response variable.

0022–5193/01/100201 + 19 $35.00/0

One approach to modeling spatial biological interactions is to treat space implicitly. Implicitly spatial "mean-field" models, which do not distinguish between different locations in space, involve the simplifying assumption that individuals are well mixed and that each is therefore equally likely to interact with individuals at any other location (Durrett & Levin, 1994). This assumption, analogous to the mass action approximation of chemistry, requires the spatial movement scale of individuals to be large compared to the spatial scale on which interactions occur and, conversely, the temporal scale of movement to be smaller than that of interactions. Most non-spatial models of biological systems that are systems of ordinary differential or difference equations fall into this category. Many of these models take the general form

$$\frac{\mathrm{d}\mathbf{f}(t)}{\mathrm{d}t} = \mathbf{R}(\mathbf{f}(t)), \tag{1}$$

where **f** and **R** are vector functions. The elements of **f** quantify the total densities of different classes of individuals as functions of time, while elements of **R** represent corresponding rates of reactions. Familiar models of this sort describe Michaelis–Menten enzyme kinetics, Lotka–Volterra population dynamics, and neural activity (Murray, 1989).

Another major approach to modeling biological systems is to treat space explicitly. By distinguishing among different locations in space, spatially explicit models can address situations in which the mass action approximation fails. Interactions in spatially explicit models are often local, with individuals interacting only between adjacent locations in space. This limitation implies that the spatial and temporal scales of movement and interaction are comparable. Reaction–diffusion equations are examples of local models that are continuous in space and in time. These familiar models typically take the form

$$\frac{\partial \mathbf{f}(x,t)}{\partial t} = \mathbf{R}(\mathbf{f}(x,t)) + \mathbf{D}\cdot\frac{\partial^2 \mathbf{f}(x,t)}{\partial x^2}, \tag{2}$$

where x is a spatial coordinate, and **f** and **R** are defined as in the spatially implicit case except for an additional explicit dependence on spatial coordinates. The second term in this equation describes dispersal of different classes of individuals, where **D** is a vector whose elements represent corresponding constant dispersal magnitudes. Reaction–diffusion-type models have a rich history in biology. Fisher (1937), Skellam (1951), and Andow *et al.* (1990) examined rates of gene and population spread using simple reaction–diffusion equations. Following Turing's (1952) initial investigation of the reaction and diffusion of chemicals important in morphogenesis, researchers have used similar equations to explain diverse examples of biological pattern formation, ranging from neurological mapping (Ermentrout & Cowan, 1979), cell alignment (Murray *et al.*, 1983; Odell *et al.*, 1981), and leaf vein formation (Mitchison, 1980) to morphological development (Murray, 1981). Mathematical biologists have applied the same types of reaction–diffusion mathematical formulations to the aggregating behavior of cells (Grindrod *et al.*, 1989; Oster & Murray, 1989) and multicellular organisms (Grindrod, 1988; Keller & Segel, 1970; Kierstead & Slobodkin, 1953; Levin & Segel, 1985; Okubo, 1980).

Non-local spatially explicit models are the focus of this paper. These are models in which interactions occur between non-adjacent locations. The presence of non-local interactions indicates that the spatial scale of movement is large and the temporal scale is small in comparison to other processes that are modeled explicitly, but not so much as for different locations to become indistinguishable. We examine the relationship between model framework and differences in processes' rates in detail in the next section. For now, we simply note that in continuous space, many non-local models take the partial integro-differential form

$$\frac{\partial \mathbf{f}(x,t)}{\partial t} = \int_{-\infty}^{\infty} \mathbf{W}(x,x')\cdot\mathbf{R}(\mathbf{f}(x',t))\,\mathrm{d}x' - \mathbf{R}(\mathbf{f}(x,t))\cdot\int_{-\infty}^{\infty}\mathbf{W}(x',x)\,\mathrm{d}x' \tag{3}$$

or the difference form

$$\mathbf{f}(x,t+1) = \int_{-\infty}^{\infty}\mathbf{W}(x,x')\cdot\mathbf{R}(\mathbf{f}(x',t))\,\mathrm{d}x'. \tag{4}$$

The definitions of x, $\mathbf{f}$, and $\mathbf{R}$ are unchanged in these equations, and $\mathbf{W}$ and $\tilde{\mathbf{W}}$ are vector functions, which are linear dispersal kernels, that gives probabilities of rates of motion from point x' to point x. Examples of non-local models are becoming more common in biology (Mollison, 1977; Kot & Schaffer, 1986; Lewis, 1994; Neubert *et al*., 1995; Mogilner & Edelstein-Keshet, 1999).

Models that express non-local interactions are useful to biologists for several reasons. Most importantly, non-local models lend themselves to the types of data biologists frequently collect. Although many biological variables of interest may be affected by processes that occur on small spatial or temporal scales, collecting sufficient data to characterize these processes may be prohibitively difficult. For example, substantial movement of seeds or of animals may take place on a time-scale of several minutes. Biologists interested in measuring individual movement, however, may collect data on the scale of hours or days by setting seed traps at given distances from individual plants, or marking animals released at one location and attempting to recapture them at varying distances from that location. Because non-local models describe the effects of small-scale processes on larger spatial scales and longer temporal scales, they provide a theoretical framework that naturally corresponds to the data that empiricists collect. Other advantages, to be explained as we develop the mathematical framework of non-local models in the next section, include an intuitive description of slower-scale processes and efficiency in numerical solution.

In the next section, we examine the scales of biological interactions, formalize scaling arguments and cover the mathematical relationship between non-local and local models. In Section 3, we apply the concepts developed in Section 2 to two concrete examples, demonstrating non-local models' potential to facilitate understanding of complex processes and to accommodate biological data. We conclude with a general discussion on non-local models' utility for biological problems.

2. Mathematical Formulation of Non-local Dynamics

To demonstrate how the relative scales of important processes can determine the appropriate form for spatial models, we develop a simple model to describe the changes in population density of a hypothetical organism. We treat individual density as the response variable of interest and individual movement as the process coupling locations across space. Individual movement is in turn mediated by a signal that is produced by the organisms themselves. Such situations are common in biology. For example, the bird cherry-oat aphid, *Rhopalosiphum padi*, forms aggregations on its winter host, *Prunus padus*, in patterns that suggest that *R. padi* individuals secrete and respond to an aggregation pheromone (Pettersson, 1993). In a similar situation, individual myxobacteria glide randomly within colonies (Dworkin & Kaiser, 1985) but begin to aggregate when starved. One proposed mechanism that can explain this behavior is that the bacteria communicate by secreting and responding to diffusing chemoattractants (Shi & Zusman, 1994). The essential feature of both the aphid system and the myxobacteria system is that changes in densities of moving individuals are mediated by signals that the individuals produce themselves. Since aggregations of aphids may enjoy greater access to plant resources (Way & Cammell, 1970) or reduced risk of predation (Turchin & Kareiva, 1989) and since aggregated myxobacteria may share some important enzymes, a model that could reliably describe aggregation in these two systems would help to elucidate important aspects of their biology. We develop a simple model for aggregation and examine the effects of separations of scale among the response, coupling, and signalling processes.

We begin with general, local, and nonlinear equations to describe changes in the density of organisms due to movement and changes in the density of signalling chemicals due to secretion and decay. Scaling analysis demonstrates that, given appropriate separations between important processes, a non-local formulation can approximate the local model. The non-local model describes changes in individual density without explicit reference to signal dynamics or detailed descriptions of individual movement. We argue that, although the two-model formulations yield the same biological predictions, non-local descriptions may provide more insight into biological systems and can be more efficient to solve

numerically. We support our qualitative arguments with numerical results and linear stability analysis.

2.1. SIMPLE MODEL OF SELF-AGGREGATION

We begin with some basic modeling approximations that are appropriate to *R. padi* and myxobacteria aggregation. Space in our model is a one-dimensional domain of length L, and both space and time are continuous. We also consider the population to be closed, with no births or deaths so that spatial changes in density are due to movement alone. We describe the population with a density function, $f(x, t)$, with dimensions *numbers of individuals per unit length*. This continuous description is valid when (i) the total number of organisms $N \gg 1$, and (ii) the average distance between neighbor organisms is much less than relevant spatial scales of the system (Lin & Segel, 1974). Both of these conditions are satisfied in the above-mentioned biological situations. We consider individuals to move by biased diffusion, which is a combination of random motion and drift:

$$\frac{\partial f(x,t)}{\partial t} = D\frac{\partial^2 f(x,t)}{\partial x^2} - \frac{\partial}{\partial x}[V(x,t)f(x,t)]. \quad (5)$$

Here D is the diffusion coefficient in dimensions *length squared per time*, and V is the drift velocity in *length per time*. Others have investigated in great detail how this continuous model can be derived from microscopic processes such as moving and turning (Alt, 1980; Othmer *et al*., 1988; Othmer & Stevens, 1997). Here we do not concern ourselves with detailed mechanisms, and we focus instead on modifying the basic advection–diffusion model to capture the relevant features of aphid or myxobacteria biology.

The rates at which individuals move in nature depend upon biological information obtained from the environment. We assume that individuals move in response to a pheromone or chemoattractant signal field $s(x, t)$ and that their movement depends on the gradient of the signal rather than on the signal's local value. This rule approximates the movement of insects or cells in the direction of higher chemical concentrations regardless of local concentration. To capture this rule, we write that the rate of deterministic drift is proportional to the spatial gradient of the signal,

$$V(x,t) = k\partial s/\partial x. \quad (6)$$

Here k is a proportionality coefficient, in dimensions *length squared per signal density per time*, which measures the sensitivity of the drift rate to the signal gradient. Meanwhile, we assume that individual movement due to stimuli other than the signal of interest is random, and represent it by a signal- and density-independent diffusion coefficient, $D = const$.

To capture the situation in which individuals produce the signal field themselves, we assume that each individual aphid or bacterial cell can produce the pheromone or chemoattractant that triggers aggregation. We postulate that the production of such a signal must therefore be proportional to the individual's density. If we assume that the signal chemical diffuses through space and decays exponentially with time, we may write the following equation to describe the change in the concentration of signal with respect to time and space:

$$\frac{\partial s(x,t)}{\partial t} = D_s\frac{\partial^2 s(x,t)}{\partial x^2} + \alpha f(x,t) - \beta s(x,t). \quad (7)$$

Here α and β are rate constants of production and decay in dimensions *signal density per individual density per time* and *per time*, respectively, and D_s is the diffusion coefficient for the signal.

Together, eqns (5–7) provide a general, closed system of nonlinear partial differential equations for a model of aggregation. We consider this model to be local because the two reaction–diffusion-type equations imply a mechanistic knowledge of how individuals and signal molecules move at every point in time and space. Biologically, realistic boundary conditions on these equations specify no flux of organisms or signal at the edges of the spatial domain, which for aphids may be a single leaf (Pettersson, 1993) and for myxobacteria *in vitro* may be a Petri dish. This model is similar to the Keller–Segel model for bacterial chemotaxis, whose solutions and properties have been extensively studied

(Childress & Percus, 1981; Mimura *et al*., 1993; Nanjundiah, 1973; Othmer & Stevens, 1997).

2.2. LINEAR STABILITY ANALYSIS

To determine when aggregation occurs in our model, we conduct a linear stability analysis of its spatially homogeneous steady state. One may verify that homogeneous distributions of organisms and signal molecules across the spatial domain:

$$f(x,t)=\bar{f}=\frac{N}{L},\quad s(x,t)=\bar{s}=\frac{\alpha N}{\beta L} \tag{8}$$

constitute a steady-state solution of model equations (5–7). Indeed, when the spatial derivatives of both distributions are equal to zero, the rate of drift of the organisms is equal to zero (6), and density changes due to diffusion stop as well. Also, at the level of the signal given by eqn (8) the rate of signal secretion is equal to the rate of decay.

Linear stability analysis answers the question of how fast small-amplitude, harmonic density profile perturbations to the homogeneous steady state grow or decay. Representing the densities in the form

$$f(x,t)=\bar{f}+\tilde{f}(x,t),\quad s(x,t)+\bar{s}+\tilde{s}(x,t),$$

where $\tilde{f}(x,t)$ and $\tilde{s}(x,t)$ are small perturbations, we substitute these expressions into eqns (5–7) and keep only terms that are linear with respect to small perturbations. We obtain the following system of linear equations:

$$\frac{\partial\tilde{f}}{\partial t}=D\frac{\partial^2\tilde{f}}{\partial x^2}-k\tilde{f}\frac{\partial^2\bar{s}}{\partial x^2}, \tag{9}$$

$$\frac{\partial\tilde{s}}{\partial t}=D_s\frac{\partial^2\tilde{s}}{\partial x^2}+\alpha\tilde{f}-\beta\tilde{s}. \tag{10}$$

The model's temporal invariance suggests the following form for the perturbations:

$$\tilde{f}(x,t)=f_0\mathrm{e}^{\lambda t}g(x),\quad \tilde{s}(x,t)=s_0\mathrm{e}^{\lambda t}g(x).$$

Substituting these expressions into eqns (9 and 10), we find that the following harmonics satisfy eqns (9 and 10) and no-flux boundary conditions:

$$g(x)=\cos(qx),\ 0\leqslant x\leqslant L,\ q=\frac{\pi j}{L},\ j=1,2,\ldots\ .$$

Since perturbations are characterized by their linear growth rate, λ, and wavelength, $2L/j$, where j represents the wavenumber, we rewrite differential equations (9 and 10) as linear algebraic equations for the amplitudes of the perturbations:

$$\lambda f_0=-Dq^2f_0+k\bar{f}q^2s_0,$$

$$\lambda s_0=-D_sq^2s_0+\alpha f_0-\beta s_0.$$

These equations have non-trivial solutions if and only if the following relation between the linear growth rate and the wavenumber is satisfied:

$$\left(\lambda+\frac{\pi^2Dj^2}{L^2}\right)\left(\lambda+\beta+\frac{\pi^2D_sj^2}{L^2}\right)-k\alpha\bar{f}\frac{\pi^2j^2}{L^2}=0. \tag{11}$$

Simple analysis shows that if the inequality

$$\frac{k\alpha\bar{f}}{\beta D}<1+\frac{\pi^2D_s}{\beta L^2}$$

holds, then at each wavenumber the linear growth rate is negative, perturbations decay, and the homogeneous steady state is stable. If the left-hand side of the inequality becomes greater than the right-hand side, however, then at small wavenumbers the linear growth rate becomes positive, perturbations start to grow, and the stability is broken. Specifically, if

$$1+\frac{\pi^2D_s}{\beta L^2}<\frac{k\alpha\bar{f}}{\beta D}<1+\frac{4\pi^2D_s}{\beta L^2},$$

then the only unstable mode of perturbation corresponds to the wavenumber $j=1$ and wavelength $2L$. In other words, under the above inequality we expect perturbations of only this mode to grow.

These results of the stability analysis lend themselves to biological interpretation. The ratio

$k\alpha\bar{f}/\beta D = k\bar{s}/D$ is the ratio of the magnitude of individuals' signal-dependent drift, $k\bar{s}$, to their diffusion via random motion. Because the quantity $k\bar{s}$ determines the magnitude of drift and carries the same dimensions *length squared per time* as diffusion coefficients, we consider it a measure of the "aggregation strength" of the system. The first inequality in the preceding paragraph thus indicates that when the aggregation strength overcomes diffusion, perturbations of the homogeneous steady-state result in aggregation. As the ratio becomes greater, we expect denser and more compact aggregations to evolve. When, as indicated by the second inequality, the aggregation strength is only slightly greater than the diffusion coefficient, we expect the resulting aggregation of individuals to be of a spatial scale comparable to the size of the finite domain, L. Thus, in the case of weak to moderate aggregation, the size of the domain is a meaningful length scale of the biological system.

2.3. SCALING ANALYSIS AND PERTURBATION THEORY

To reveal important relationships between the scales of processes relevant to aggregation, we perform a non-dimensionalization of our local model. The first step in the non-dimensionalization is to choose an appropriate unit of time. Since the purpose of our modeling effort is to understand the grouping behavior of individuals, the chosen unit should be relevant to changes in individual density rather than to changes in signal density. The two processes that directly affect individual density are random diffusion and signal-dependent advection. We restrict our attention to the case in which the rates of these two processes are comparable, with aggregative drift only slightly greater than diffusion. In this case, as we showed in the preceding section, the size of the aggregation that results is on the scale of the domain size L. Thus, an appropriate choice of temporal unit for the development of aggregation is the characteristic time for an individual to drift or diffuse across the spatial domain: $T = L^2/D$.

The constant steady-state densities of the organisms and the signal, $\bar{f}$ and $\bar{s}$, are natural choices for their characteristic densities. Given these choices and the temporal unit T, we introduce the non-dimensional quantities:

$$x' = \frac{x}{L}, \quad t' = \frac{t}{T} = \frac{Dt}{L^2},$$

$$f' = \frac{f}{\bar{f}} = \frac{Lf}{N}, \quad s' = \frac{s}{\bar{s}} = \frac{\beta Ls}{\alpha N},$$

which enable us to re-write nonlinear model equations (5–7) in the non-dimensional form:

$$\frac{\partial f'}{\partial t'} = \frac{\partial^2 f'}{\partial x'^2} - k' \frac{\partial}{\partial x'}\left[f' \frac{\partial s'}{\partial x'} \right], \quad k' = \frac{k\alpha\bar{f}}{\beta D}, \tag{12}$$

$$\varepsilon_1 \varepsilon_2 \frac{\partial s'}{\partial t'} = \varepsilon_2 \frac{\partial^2 s'}{\partial x'^2} + (f' - s'), \quad \varepsilon_1 = \frac{D}{D_s}, \quad \varepsilon_2 = \frac{D_s}{\beta L^2}. \tag{13}$$

Equations (12 and 13) show that the values of the dimensionless parameters k', ε_1, and ε_2 completely determine the behavior of the model. Since each of these three ratios represents a comparison between the rates of two processes, an investigation of their magnitudes sheds light on the relative scales of those processes. The parameter k' coincides with the ratio of the aggregation strength to diffusion that appeared in the linear stability analysis, so under conditions of moderate aggregation $k' \sim 1$. To determine reasonable values of ε_1 and ε_2, we return to our two illustrative examples.

The parameter ε_1 is a dimensionless quantity that compares the rate of organisms' diffusion with the rate of the signal's diffusion. In the case of myxobacteria, the effective diffusion coefficient of the cells is of the order of magnitude $D \sim 10^{-9}\,\mathrm{cm^2\,s^{-1}}$ (estimated using data from (Spormann & Kaiser, 1995)), while the diffusion coefficient of chemoattractants in an aqueous environment is typically on the order of $D_s \sim 10^{-5}\,\mathrm{cm^2\,s^{-1}}$ (Weast *et al.*, 1983, p. F-46). A reasonable effective diffusion coefficient characterizing the random motion of aphids is $D \sim 1\,\mathrm{cm^2\,s^{-1}}$ (estimated using data from Pettersson, 1993), while the estimated diffusion coefficient of pheromones in the air is $D_s \sim 0.1\,\mathrm{cm^2\,s^{-1}}$ (Weast *et al.*, 1983, p. F-46). Thus, in both of our biological examples, $\varepsilon_1 \ll 1$ ($\varepsilon_1 \sim 0.0001$ for bacteria,

and $\varepsilon_1 \sim 0.1$ for aphids). In biological terms, the smallness of ε_1 indicates that *the motion of the signal is much faster than the motion of individuals.*

If we write the dimensionless parameter ε_2 in the form: $\varepsilon_2 = \beta^{-1}/(L^2/D_s)$, its meaning as the ratio of the signal chemical's half-life time to the characteristic time for the chemical to diffuse across the spatial domain is clear. The latter time is of the same order of magnitude for both biological systems: in the experiments with myxobacteria, $L \sim 1$ cm and $L^2/D_s \sim 10^5$ s, and in the aphid case, $L \sim 100$ cm and $L^2/D_s \sim 10^5$ s. Thus, if the value of $\beta^{-1} \ll 10^5$ s $\simeq 1$ day, which is reasonable to assume in both cases, then $\varepsilon_2 \ll 1$. The interpretation of this inequality is that the signal decays well before it can diffuse across the spatial domain, so *boundary conditions have little influence on the dynamics of the signal.*

With knowledge of the magnitudes of parameters ε_1 and ε_2 in hand, we identify a quantitative hierarchy of the three terms in eqn (13). If our choices for the characteristic temporal and spatial scales were appropriate, which can only be justified *a posteriori*, then the last term on the right-hand side is on the order of unity. The first term on the right-hand side is much smaller, on the order of $\varepsilon_2 \ll 1$. Finally, the left-hand term is smaller still, on the order of $\varepsilon_1\varepsilon_2 \ll \varepsilon_2$. Because this term is so small, we can neglect it according to "naive" perturbation theory (Lin & Segel, 1974), thereby simplifying the model considerably. Biologically, such a simplification is justified because the smallness of the left-hand term in eqn (13) means that the dynamics of the signal are very fast. After brief signal transients decrease, therefore, dynamic changes in the signal are negligible.

Using this reasoning, can we simplify our model further by also neglecting the small diffusion term in eqn (13)? Doing so implies that very little of the information about signal dynamics is relevant, and that signal density simply reflects the density of the organisms without any appreciable difference in the rates of the two processes: $s' = f'$. We would then obtain the following closed, local equation for the density of the organisms:

$$\frac{\partial f'}{\partial t'} = \frac{\partial^2 f'}{\partial x'^2} - k' \frac{\partial}{\partial x'}\left[f' \frac{\partial f'}{\partial x'}\right].$$

This equation, however, is ill-posed mathematically, which becomes clear from the linear stability analysis. Substituting a perturbed density of the form $f'(x', t') = 1 + f_0 e^{\lambda' t'} \cos(\pi j x')$ into this equation and linearizing with respect to the small perturbation amplitude f_0, we obtain the dispersion relation: $\lambda' = (k' - 1)(\pi j)^2$. In the biologically interesting situation when aggregation takes place, $k' > 1$, so $\lambda' \to \infty$ as $j \to \infty$, or $(L/j) \to 0$. This calculation means that small-wavelength perturbations grow infinitely fast, which is biologically unrealistic.

To understand why neglecting the signal's diffusion term invalidates the model, consider a signal inhomogeneity of spatial scale δ. This inhomogeneity generates local organismal drift with a rate on the order of $V \sim k\bar{s}/\delta$. This drift causes an inhomogeneity in the distribution of the organisms of spatial scale $D/V \sim (D/k\bar{s})\,\delta = \delta/k'$. In cases when aggregation takes place and $k' > 1$, this result means that the spatial scale of perturbations to the density of the organisms, δ/k', is less than that of perturbations to the signal, δ. Without signal diffusion, the signal dynamics lose their spatial dimension, which formally means that their spatial scale becomes equal to zero. To be consistent, the spatial scale of the organism's density must also be equal to zero, which implies that a spatially explicit model is inappropriate for this system.

Mathematically, this phenomenon indicates that a small signal diffusion term is a singular, rather than regular, perturbation of the signal kinetics (Lin & Segel, 1974). Indeed, one may verify that the regular perturbation series $s' = f' + \sum_{i=1}^{\infty} \varepsilon_2^i (\mathrm{d}^{2i} f'/\mathrm{d}x'^{2i})$, which can be obtained from the equation $\varepsilon_2(\mathrm{d}^2 s'/\mathrm{d}x'^2) + (f' - s') = 0$, is not asymptotic, meaning that the corresponding local approximation is not valid. One of the ways to solve this singular perturbation problem is to attempt a *non-local approximation of the local nonlinear model* (12 and 13).

2.4. NON-LOCAL APPROXIMATION

Returning to the full non-dimensional model (12 and 13), we examine the validity of retaining the signal's diffusion term but neglecting the much smaller term on the left-hand side of eqn (13). As explained in the previous section,

this simplification is justified biologically by the fact that signal movement is much faster than individual movement. After taking advantage of this separation of scales between the two movement processes, we can solve the simplified linear ordinary differential equation for the signal's spatial distribution, $\varepsilon_2(\mathrm{d}^2s'/\mathrm{d}x'^2) - s' = f'$, *on an infinite domain* using the Green's functions technique (Morse & Feshbach, 1953, Chapter 7):

$$s'(x') = \int_{-\infty}^{\infty} \mathrm{d}x'' G(x' - x'') f'(x''),$$

$$G(d) = \frac{1}{2\sqrt{\varepsilon_2}} \exp\left(-\frac{|d|}{\sqrt{\varepsilon_2}}\right). \tag{14}$$

Since we are concerned with a finite domain, we must use a different Green's function G than this one for an infinite domain. In the case when $\varepsilon_2 \ll 1$, however, which means that the domain's boundaries have little effect on the signal's distribution, we can consider the desired finite-domain Green's function to be a small perturbation of the function given for the infinite domain (Morse & Feshbach, 1953). We can then approximate the signal distribution as follows:

$$s'(x') \simeq \frac{1}{2\sqrt{\varepsilon_2}} \int_0^1 \mathrm{d}x'' \exp\left(-\frac{|x' - x''|}{\sqrt{\varepsilon_2}}\right) f'(x'').$$

The model equation for the motion of the organisms assumes the closed non-local form:

$$\frac{\partial f'}{\partial t'} = \frac{\partial^2 f'}{\partial x'^2} - \frac{\partial}{\partial x'}\left[V'(x')\frac{\partial s'}{\partial x'}\right], \tag{15}$$

$$V'(x') \simeq \frac{-k'}{2\varepsilon_2} \int_0^1 \mathrm{d}x'' \,\mathrm{sign}(x' - x'') \times \exp\left(-\frac{|x' - x''|}{\sqrt{\varepsilon_2}}\right) f'(x''). \tag{16}$$

This spatially non-local model describes density changes as a result of direct, long-distance interactions between individuals without reference to the signal. We have used a separation of scales between the rates of signal movement and individual movement to eliminate information that is unimportant to the larger-scale processes of interest.

The linear stability analysis of the spatially non-local model (15 and 16) is difficult on the finite domain, but is much simpler on an infinite domain. The infinite-domain result is relevant to the finite domain because the boundary conditions should not affect the aggregation behavior strongly. Substituting a density of the form $f'(x, t) = 1 + f_0 \mathrm{e}^{\lambda' t'} \cos(qx')$ into eqns (15 and 16), where q is a continuous wave vector playing the role of a discrete wave number and where the limits of integration are infinite, we discard terms not linear with respect to the small perturbation amplitude f_0 to obtain the dispersion relation,

$$\lambda(q) = -q^2 + \frac{k'q^2}{q^2 + 1}.$$

This relation gives approximately the same instability criterion as the original model: $k' > 1$. At such values of k', the linear growth rate is positive for small values of the wave vector, so aggregation should occur on large spatial scales. Therefore, system (15 and 16) is an adequate approximation for the original system (12 and 13). Furthermore, as in the original local model, at large values of the wave number the linear growth rate is negative and proportional to the square of the wave number. This demonstrates the quick decay of small-wavelength perturbations, which indicates that the non-local approximation is well posed: small-scale fluctuations in the density become insignificant, rather than growing so large as to dominate the models' behavior.

The simplified non-local system (15 and 16) offers an advantage over the local system (12 and 13) in the form of a clear picture of apparently direct interactions between individuals. Avoiding explicit reference to the very fast dynamics of the signal that mediates interactions allows eqns (15 and 16) to provide an intuitively satisfying expression of interactions on a slower scale. For example, expression (16) explicitly demonstrates the attraction, or convergence, between individuals at locations x' and x''. The only factor that influences the sign of the velocity of the

individual at x' is the sign of $(x' - x'')$, so that if $x' > x''$, then the velocity is negative and x' decreases. On the other hand, if $x' < x''$, then the velocity is positive and x' increases. In both cases, the distance $|x' - x'|$ diminishes, indicating convergence between individuals. Because of the negative exponential term in eqn (16), the rate of this convergence realistically decreases exponentially with increasing distances between locations. This information is more difficult to obtain from the local system of equations (12 and 13), making the non-local system (15 and 16) a natural choice for describing the biology of aggregation.

A second advantage of non-local equations is that they may be easier to solve numerically because they take advantage of separations of scale. To demonstrate this point, we solved the dimensionless non-local equation (15) numerically, with no-flux boundary conditions and using the explicit forward-time centered-space finite difference scheme (Garcia, 1994). We discretized the domain of unit length with 20 grid points, and used parameter values $k' = 1.3$ and $\varepsilon_2 = 0.1$. At each time step we computed the convolution integral (16) numerically using the composite trapezoidal rule. The density profile illustrated in Fig. 1 evolved within 0.5 time units under various initial conditions. The profile shows that individuals aggregate at the center of the domain, forming a group of a size comparable to the size of the domain. These results are in agreement with the predictions of the stability and scaling analyses. The numerical procedure used to solve the non-local equation was stable at time steps as large as 0.005 time units. Meanwhile, a numerical solution of the corresponding local system of equations (12 and 13) using the same finite difference scheme and $\varepsilon_1 = 0.1$ gave similar results only with time steps that were one to two orders of magnitude smaller. This difference in stability results from the fact that the signal changes on much faster time-scale than the density of the individuals, so a smaller time step is required to solve a model that explicitly includes signal dynamics. Since the computation of the convolution integral (16) in the non-local model can be programmed in a vector form that does not increase total computational time, the non-local model provides an order-of-magnitude improvement in total computational time over the local model.

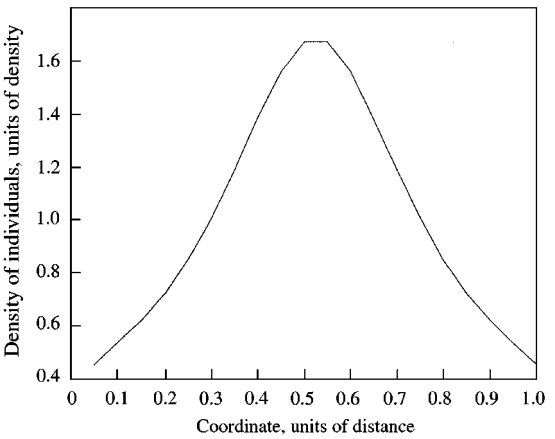

FIG. 1. The solid line shows the steady-state density of individuals in the non-local self-aggregation model that evolves from random initial conditions. We used the conserved average initial density as the unit of density, and the length of the spatial domain as the unit of distance.

In this section, we showed that a simplified, non-local model adequately captures the behavior of a full, local model when some process is sufficiently fast compared to the process of primary biological interest. Thus, whereas a local model specifies mechanistic detail about all processes that interact in a given system, a non-local model represents only the effects of fast processes on the scale of a slower one. In the next section, we show how this encapsulation of fast processes helps non-local models to accommodate biological data.

3. The Relationship between Mathematical Formulations and Biological Data

We use two concrete examples, one from cellular biology and one from animal behavior, to demonstrate that non-local models are a particularly convenient theoretical framework for the types of data that biologists often collect and the kinds of questions they often ask.

3.1. SELF-ORGANIZATION OF THE CYTOSKELETON

Microtubules are long protein fibers found in all eukaryotic cells (Bray, 1994). An important part of the cytoskeleton, microtubules provide

lines of transport, communication, and control in the cell and also organize cell movements. In a typical animal cell, for instance, microtubules radiate from a position close to the nucleus to the cell periphery. In association with a cytoplasmic protein called dynein, these microtubule asters help move organelles from the cell's periphery to its center. In an aster, microtubules are arranged with their negatively charged "minus" ends embedded in a centrosome and their positively charged "plus" ends stabilized at the cell membrane. The organelle-carrying dynein molecules contain a "head" of ATPase that uses the energy of hydrolysis to move along microtubules toward the minus ends, resulting in organelle motion toward the cell's center (Bray, 1994).

A very fine microsurgical procedure recently demonstrated that the presence of dynein molecules may also contribute to the organization of microtubule structures. Researchers cut an oblong fragment from the periphery of a fish melanophore cell (Rodionov & Borisy, 1997). The fragment contained microtubules and pigment-containing granules that are associated with dynein molecules. To rule out the competing hypothesis that the centrosome organizes aster formation, however, the fragment contained no centrosomal material. Although the pigment granules associated with dynein motors were originally distributed in the fragment with uniform density, they gradually aggregated at the edge of the fragment that had been closer to the nucleus before the microsurgical procedure. Similarly, the microtubules' minus ends did not remain distributed throughout the fragment but instead accumulated at the same edge of the fragment as the granules. Later, the aggregate of the granules started to move slowly to the center of the fragment, but here we do not attempt to model or explain this slow self-centering process.

This example of *in vitro* self-organization suggests a hypothesis for the formation of *in vivo* cytoskeletal structure. Dynein motors aggregate towards microtubules' minus ends. Microtubules cannot move because they are crosslinked into a meshwork of actin. Apparent motion occurs, however, as the asymmetric globular subunits of the polymer assemble to and disassemble from the plus and minus ends of the microtubule. This process causes microtubules' plus ends to grow and minus ends to shrink, so that the fibers *treadmill* with an overall appearance of translational movement toward the plus ends (Bray, 1994). In the presence of dynein motors, minus ends disassemble more slowly than plus ends assemble, with rate $V_m < V_p$. If, as in the experiment with fish melanocytes, the polymers are initially oriented with their minus ends to the left and their plus ends to the right, the movement of the dynein molecules slows the disassembly of minus ends at the left and increases their concentration there. This, in turn, causes even greater aggregation of the dynein molecules, further increasing the concentration of the minus ends. If dynein molecules can also initiate the assembly of new microtubule fibers, the described positive feedback loop could provide a qualitative explanation for minus-end anchoring near the nucleus. Using the techniques outlined in the previous section, we develop a non-local model to explore this hypothesis in more detail. We demonstrate that a model that takes advantage of separations of scale between important processes yields valuable biological predictions.

3.1.1. *Local Model of Dynein-mediated Microtubule Organization*

We describe the cell–fragment system on the one-dimensional domain $0 < x < L$ by the densities of the dyneins and microtubule plus and minus ends, $d(x, t)$, $p(x, t)$ and $m(x, t)$, respectively. The equations for plus and minus end densities have the form:

$$\frac{\partial p}{\partial t} = -V_p \frac{\partial p}{\partial x} + nd, \tag{17}$$

$$\frac{\partial m}{\partial t} = -\frac{\partial}{\partial x}(V_m m) + nd, \tag{18}$$

where the first term describes the drift of the plus and minus ends due to assembly and disassembly, respectively. The second term describes nucleation of plus and minus ends. Since the nucleation of a fiber is a simultaneous appearance of plus and minus ends in the same place, the rates of change of the two kinds of ends due to nucleation are equal. Because we assume that dyneins cause nucleation, the nucleation rate is

proportional to the dynein density with corresponding proportionality coefficient n. We describe the dynamics of dynein density with the advection–diffusion equation:

$$\frac{\partial d}{\partial t} = \frac{\partial}{\partial x}(V_d d) + D\frac{\partial^2 d}{\partial x^2}, \tag{19}$$

where V_d is the rate of directional drift of the motors to the left, toward microtubule minus ends, and D is the constant diffusion coefficient characterizing the effectively random motion of the pigment particles associated with the dynein molecules.

To complete the model, we need constitutive relations for the non-constant velocities V_d and V_m. The effective net disassembly rate of the minus ends decreases monotonically as the density of the dynein molecules increases:

$$V_m = V_p \exp(-d/\tilde{d}). \tag{20}$$

This rate is equal to V_p at $d = 0$, decreases significantly with decreases in dynein density on the order of $\tilde{d}$, where $\tilde{d}$ is a parameter for this characteristic dynein density, and approaches zero at $d \to \infty$. Meanwhile, a reasonable assumption about the velocity of the dynein motors V_d is that it depends on the local *length density* of microtubules, $l(x, t)$. When microtubules are abundant, dynein's velocity saturates to its maximal value, $\bar{V}_d$. When microtubules are absent, there are no "tracks" for motors to move on, and the motors' drift velocity drops to zero. The phenomenological expression:

$$V = \bar{V}_d(1 - \exp(-l/\tilde{l})), \tag{21}$$

where $\tilde{l}$ is the parameter for a characteristic microtubule length density, accounts for these features of the dynein motion.

Having introduced the new dynamic variable $l(x, t)$, we must now derive an equation for its changes with time. Over the time interval dt, p plus ends moving to the right with speed V_p "deposit" new total microtubule length $V_p\,dt$. At the same time, m minus ends moving to the right with speed V_m "annihilate" a previously existing length $V_m\,dt$. Then, the rate of change of the microtubule's length density is simply

$$\frac{dl}{dt} = V_p p - V_m m. \tag{22}$$

Equations (17–22), together with initial and boundary conditions specifying no plus or minus ends at the left edge of the fragment and no flux of dynein density across either edge:

$$p(0, t) = 0, \quad m(0, t) = 0, \tag{23}$$

$$V(0, t)d(0, t) + D\frac{\partial d(0, t)}{\partial x}$$

$$= V(L, t)d(L, t) + D\frac{\partial d(L, t)}{\partial x} = 0, \tag{24}$$

complete the mathematical description of the microtubule–dynein system.

3.1.2. *Scaling Analysis and Non-local Model*

The purpose of modeling the microtubule–dynein system is to try to understand cytoskeletal dynamics, which occur on a much slower temporal scale than the motion of the dynein motors: $\bar{V}_d \sim 1\ \mu m\,s^{-1} \gg V_p \sim 0.1\ \mu m\,s^{-1}$. Thus, to focus on microtubule organization, we non-dimensionalize equations (17–22) by choosing characteristic length and time units to correspond to the relatively slower rate. For instance, we choose the size of the fragment, L, as the natural unit of length, with corresponding temporal unit $T = L/V_p$ being the time needed for a fiber to treadmill across the fragment. Since the density of the dynein molecules was initially constant in the fish melanophore experiment, we choose a constant density, $d(0, t) = \bar{d}$, for the characteristic density of dynein. To obtain characteristic plus and minus end densities, we balance the total nucleation rate, which is of order $n\bar{d}L$, with plus and minus end fluxes out of the right edge of the fragment of order $V_p\bar{p}$ and $V_p\bar{m}$, respectively. While the ends of the immobile microtubules do not actually move across the boundaries of the fragment, an effective flux of plus ends occurs as polymerization-inhibiting proteins stabilize plus ends at the cell membrane. Similarly, an apparent flux of minus ends occurs when fibers' minus ends

approach the membrane and the entire fiber disappears. We balance these processes with the creation of new fibers to obtain the characteristic densities $\bar{p} = \bar{m} = n\bar{d}L/V_p$. Finally, the scale of the microtubule's length density can be estimated as the scale of the rate of the length density change, $V_p\bar{p}$, times the characteristic time scale: $\bar{l} = n\bar{d}L^2/V_p$.

Introducing the non-dimensional variables

$$x' = x/L, \quad t' = t/T, \quad d' = d/\bar{d}, \quad p' = p/\bar{p},$$

$$m' = m/\bar{m}, \quad l' = l/\bar{l},$$

assuming for simplicity that $\tilde{l} = \bar{l}$ and $\tilde{d} = \bar{d}$, and dropping prime signs for convenience, we arrive at the non-dimensionalized system of equations:

$$\varepsilon\frac{\partial d}{\partial t} = \frac{\partial}{\partial x}(vd) + a\frac{\partial^2 d}{\partial x^2}, \quad v = 1 - e^{-l},$$

$$a = \frac{V_p D}{\bar{V}_d^2 L}, \quad \varepsilon = \frac{V_p}{\bar{V}_d} \ll 1, \tag{25}$$

$$\frac{\partial p}{\partial t} = -\frac{\partial p}{\partial x} + d, \tag{26}$$

$$\frac{\partial m}{\partial t} = -\frac{\partial}{\partial x}(v_m m) + d, \quad v_m = \mathrm{e}^{-d}, \tag{27}$$

$$\frac{\mathrm{d}l}{\mathrm{d}t} = p - v_m m. \tag{28}$$

We focus on the case where the dimensionless parameter $a \sim 1$, meaning that the rate of random dynein movement is of the same order of magnitude as the maximum motor speed. As in Section 2, the smallness of the parameter ε in front of the time derivative of the dynein density suggests that we may use arguments of perturbation theory to neglect the dynein dynamics. Biologically, this neglect is justified because the distribution of dynein is expected to reach a quasi-steady state on the fast time-scale, $L/\bar{V}_d$. The quasi-steady state is determined implicitly by the microtubule's length density, which changes on the slow time-scale, L/V_p. We can find the quasi-steady dynein distribution from the equation:

$$\frac{\mathrm{d}}{\mathrm{d}x}\left[(1 - \mathrm{e}^{-l})d + a\frac{\mathrm{d}}{\mathrm{d}x}(d)\right] = 0.$$

Integrating this equation once, taking into account the fact that the flux of the dynein molecules has to be equal to zero in an equlibrium, and integrating a second time, we obtain the quasi-steady dynein density in the dimensionless form:

$$d(x) \simeq \frac{\exp(-a[\int_0^x \mathrm{d}y(1 - \mathrm{e}^{-l(y)})])}{\int_0^1 \mathrm{d}x\{\exp(-a[\int_0^x \mathrm{d}y(1 - \mathrm{e}^{-l(y)})])\}}. \tag{29}$$

The denominator in expression (29) is a normalization constant. The numerator contains the non-local expression for the quasi-steady dynein distribution in terms of slow-scale changes in microtubule length density. Together with eqns (26–28), this equation for the dynein density constitutes a non-local formulation for the original local model (25–28).

The non-local system (26–29) is more helpful from a biological point of view than the original local model because it expresses dynamics in terms of readily measurable quantities. For example, dynein dynamics occur on what may be an unmeasurably fast time-scale. Using the separation of scale between dynein dynamics and microtubule movement; however, we avoid detailed descriptions of fast, complex-behavior and obtain eqn (29), which gives us a qualitative understanding of the motors' behavior. Because the exponential factor in the integrand is less than one, the dynein density is a decreasing function of distance from the left end. This decrease indicates aggregation of the dynein molecules at the left, which agrees with observations of the slow-scale distribution of dynein. Moreover, as the dynein density is low everywhere except at the very left edge of the fragment, the effective minus end drift rate $v_m \simeq 1$, and according to eqn (28), $l \simeq const$ across the domain. This indicates an exponential decay of the dynein density away from the left edge of the fragment. Thus, the non-local model provides helpful analytical information about the dynein distribution that we can easily compare to experimental results.

Besides this useful qualitative information, the non-local model

$$\frac{\partial p}{\partial t} = -\frac{\partial p}{\partial x} + d, \quad \frac{\partial m}{\partial t} = -\frac{\partial}{\partial x}(\mathrm{e}^{-d}m) + d,$$

$$\frac{\mathrm{d}l}{\mathrm{d}t} = p - \mathrm{e}^{-d}\mathrm{m}, \quad p(0,t) = m(0,t) = 0, \qquad (30)$$

where d is given by eqn (29), offers a computational advantage because we can concentrate on the microtubule's dynamics on the slow timescale. We solved the dimensionless system of equations (30) numerically on the unit-length domain discretized into 20 intervals. We used the downwind finite difference scheme for the hyperbolic equations, and the forward Euler method of integration for all equations (Garcia, 1994). The integrals in eqn (29) were computed at each step of integration with the composite trapezoidal rule. We used the initial conditions $p(x,0) = m(x,0) = l(x,0) = 0$. The density profiles shown in Fig. 2 evolved within 10 time units. These numerical results agree with experimental observations of the aggregation of the dynein molecules and microtubule's minus ends at the left edge of the fragment. The numerical procedure was stable with time steps as large as 0.01 time units. Similar numerical analysis of the original local model (25–28) gave similar results only with time steps of an order of magnitude less, significantly increasing the time needed for computation.

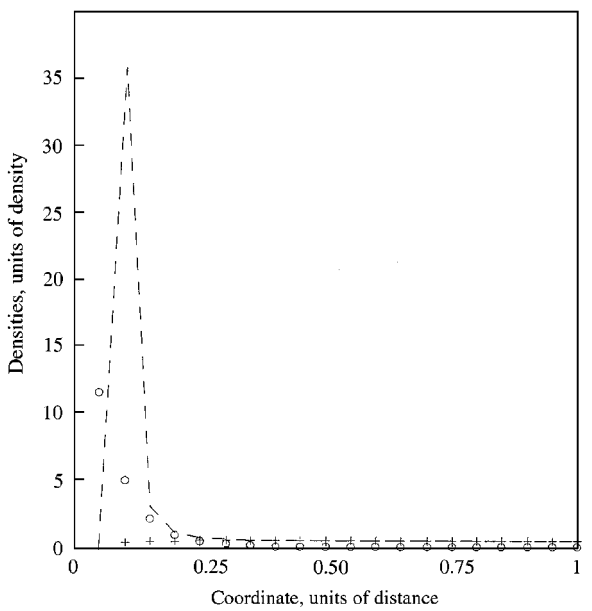

FIG. 2. Symbols indicate the asymptotically stationary concentrations of dynein molecules (○) and minus (−) and plus (+) ends of microtubules computed from the non-local cellular model. Minus ends and dynein motors aggregate at the left edge of the domain. Units of density are introduced in the text. The length of the spatial domain was used as the unit of distance: (−) density of minus ends; (+) density of plus ends; (○) density of dynein molecules.

Having shown how the techniques we developed in Section 2 help us to derive a non-local model that conveniently describes microtubule organization, we now show how non-local models can help us understand a complex problem in animal behavior.

3.2. COORDINATION OF PRIMATE GROUPS USING CONTACT CALLS

Some species of social primates emit quiet, frequent vocal calls during the course of daily activities. Early researchers conjectured that these "contact calls" promote group cohesion and coordination (Gautier & Gautier, 1977; Lindburg, 1971). More recently, researchers have explicitly addressed the question of whether or not primates use contact calls to regulate intragroup spacing (Robinson, 1982; Palombit, 1992). Robinson (1982) investigated the effects of three acoustically intergrading types of spacing-dependent calls in wedge-capped capuchins, *Cebus nigrivittatus*. He found that the capuchins emit *heh* calls when crowded, *arrawh* calls when separated, and *huh* calls at intermediate spacing. Following *hehs*, neighboring individuals generally move away from the calling individual; following *arrawhs*, they move toward it. Meanwhile, Robinson found that *huhs* have no statistically significant effect on group spacing unless they are unusually frequent, in which case neighbors tend to move toward the focal animal. Robinson (1982) concluded that vocal communication does help to maintain intragroup spacing.

Detailed information about how primates gather, process, and respond to auditory cues is scarce because it is difficult to obtain. Since experimentally establishing the importance of vocal communication in maintaining group spacing is likewise difficult, a simple model that demonstrates whether auditory cues alone can plausibly

mediate group cohesion would be a useful tool in understanding primate behavior. Such a model would treat contact calls as the signal that organizes individual movement. Acoustic information about the calls suggests that they propagate through space much faster than animals can move, since the sound of a call covers tens of meters in a tenth of a second. Meanwhile, although Robinson (1982) does not explicitly specify the scale of the capuchins' movement, the way in which he scores changes in group spacing clearly indicates that they move on the spatial scale of meters and temporal scale of seconds. Since we can therefore safely assume that the signal propagates quickly relative to animal movement, the maintenance of group cohesion via vocal communication is a promising candidate for non-local modeling.

A discrete, individual-based modeling framework is more appropriate to capuchin aggregation than a density-based approach because the number of individuals in a primate troop does not exceed 20 or 30 animals (Robinson, 1982). Within the individual-based framework, we introduce the simplest possible equation for the motion of a group in one dimension:

$$\frac{\mathrm{d}x_i}{\mathrm{d}t} = V(x_i), \quad i = 1, \ldots, N, \tag{31}$$

where t is the time, x_i is the coordinate of the ith animal, N is the number of primates under consideration, and $V(x_i)$ is the rate of motion of the ith animal at position x_i. One of the assumptions underlying eqn (31) is that the animals respond to the signal by adjusting their rate of motion rather than their acceleration, as is assumed in many individual-based models (Warburton & Lazarus, 1991). Secondly, the model formulation implies that individual motion has a continuous character. Although monkeys may move by taking discrete steps, this assumption is reasonable if the average step size is much smaller than both the average distance between animals and the characteristic size of the whole group (Jäger & Segel, 1992).

Individual velocity depends on the signal, s, which in turn depends on spatial location: $V(x_i) = V(s(x_i))$. Since we lack information about how individuals process the signal, we avoid specifying any functional dependence of movement on the variable s. We do assume, however, that movement is memoryless with respect to the signal: current levels of signal, not a weighted average of signals received prior to a response, determine rates of motion. We also assume that the time individuals require to process the signal is negligible. We know, however, that the signal propagates quickly relative to the speed of capuchin's motion: $\bar{V} \ll c$, where c is the velocity of sound and $\bar{V}$ is the order of magnitude of the capuchins' speed.

The natural length scale L in this situation is the characteristic distance between the animals. Given our assumptions that signal processing is instantaneous and memory free, two characteristic temporal scales emerge: one fast, L/c, which is the time for the signal to propagate between neighbors, and one slow, $L/\bar{V}$, representing the time needed for an animal to approach a neighbor. When we choose the scale of animal movement as the characteristic time-scale of the system, we can ignore the term describing the signal's time derivative because its order of magnitude is proportional to the small parameter $(\bar{V}/c)$. Thus, we use a separation of scale to eliminate the temporal dynamics of the signal.

Having simplified the model, we no longer concern ourselves with short-term changes in the signal. Instead, we now consider the function describing the effective signal "field" that individuals generate. As the form of the argument of this function should reflect the translational invariance of the system, we introduce the function $S(x - x_j, x_i - x_j)$, which describes the amount of signal produced by the jth individual. Because the jth individual, located at position x_j, produces signal in response to the presence of the ith individual at position x_i, the resulting amount of signal at x depends on the distance $x_i - x_j$ as well as the distance $x - x_j$. The signal produced by the jth individual that is perceived by the ith individual is therefore $S(x_i - x_j,\ x_i - x_j)$ or simply $\tilde{S}(x_i - x_j)$. Thus, the ith individual's velocity, which results as a response to this signal, depends on the distance between the animals: $V(x_i) = V(\tilde{S}(x_i - x_j)) = \tilde{V}(x_i - x_j)$. This reasoning shows clearly that the rate of motion of each individual depends on the positions of other

animals. Because we effectively eliminated the signal from the model on the slow time-scale, the equations of motion are now non-local

The non-local character of the equations for call-dependent changes in velocity is a helpful improvement over the original, local model. We cannot specify a function for velocity because mechanistic information about how vocalizations affect capuchin movement is unavailable. Our elimination of signal dynamics, however, reveals that on the time-scale of interest, each individual's velocity depends only on the positions of other individuals. This dependence corresponds nicely to the kinds of observations behavioral scientists make in the wild. Thus, we can use qualitative observations from Robinson (1982) to postulate the form of the function $\tilde{V}(x)$:

(1) The direction of the responding individual's motion depends on its direction relative to the calling individual, while the distance moved depends only on the distance between the two animals. In other words, if the positions of the caller and the respondent were exchanged, the respondent would move the same distance as previously but in the opposite direction. This situation requires that $\tilde{V}$ be odd, such that $\tilde{V}(x) = -\tilde{V}(-x)$.
(2) If the initial distance between animals is small, then *heh* calls lead to the animals' divergence. This condition requires that $\tilde{V}(x) > 0$ when x is small and positive.
(3) If the initial distance between animals is large, then *arrawh* or *huh* calls lead to convergence, and the sign of $\tilde{V}(x)$ is negative at sufficiently large positive x.
(4) When the distance between capuchins is very large, individuals do not perceive the sounds that others make. Interactions over suffciently large distances are absent because individuals move a distance $\tilde{V}(x) = 0$ in response to calls they cannot hear.

One of the simplest functions $\tilde{V}(x)$ satisfying requirements (1)–(4) is

$$\tilde{V}(x) = \begin{cases} R\,\mathrm{sign}(x), & |x| \leqslant r, \\ -A\,\mathrm{sign}(x), & a_1 \leqslant |x| \leqslant a_2, \\ 0, & \text{otherwise}, \end{cases} \qquad (32)$$

where $r < a_1 < a_2$. The parameters R and A govern the amplitude of divergent and convergent animal motion, respectively. The parameter r describes the range of distances over which repulsive interactions are significant. Between r and a_1, animals maintain "comfortable" distances among themselves: when a caller is at such a distance from a respondent, the respondent's motions are too small to be detected. If individuals are farther apart than a_1, they start to converge. Beyond the distance a_2 there is no response. We also allow a certain amount of randomness in the distance that individuals move in response to calls by adding a normally distributed random variable to the right-hand side of eqn (31).

In order to translate this description of individual behavior to a description of the movements of a whole troop, we make an assumption about how individuals respond to many calling animals at different distances. The simplest such assumption is that individuals add up the signals they receive from different animals in a linear fashion. This assumption is probably a gross oversimplification of complex decision-making processes on the part of the capuchins, but is a reasonable first step given the absence of other information. The assumption allows us to write the following nonlinear, spatially non-local model for the aggregations of capuchins:

$$\frac{\mathrm{d}x_i}{\mathrm{d}t} = \sum_{j=1}^{N} \tilde{V}(x_i - x_j) + \text{random terms}, \quad i = 1, \ldots, N, \qquad (33)$$

where the function $\tilde{V}$ is given by eqn (32).

Numerical analysis of this model yields some interesting predictions about capuchin aggregation, such as the expected troop density and the distribution of distances between animals. From the data in Robinson (1982) we find that $r \simeq 10$ m, $a_1 \simeq 20$ m, and $a_2 \simeq 100$ m. Unfortunately, however, information about the parameters R and A and the amplitude of random terms is lacking. In our simulations, therefore, we varied the parameters R and A and the amplitude of random terms. We solved eqns (32 and 33) using the forward Euler method. We assigned the

initial positions of $N = 20$ individuals randomly, and ran simulations until the average distance between the animals and the sizes of groups stopped changing. We found that the absolute values of R and A do not affect the process of aggregation significantly as long as the value of the divergence amplitude, R, is much greater than that of convergence, A. Otherwise, animals "collapse" into a very dense group. The results of one of the numerical runs of the model are shown in Fig. 3. This figure shows that the initial size of the group, about 400 m from end to end, decreased to only 225 m. The average distance between neighbors in the group became stable at about 10 m. Two individuals venturing away from the group (the one initially at position 350 m, more than 60 m away from the group, and the one left behind at position -50 m between 15 and 30 time units) were attracted back to the group. On the other hand, five individuals initially crowded between -26 and 8 m, with average distance between neighbors less than τ, quickly diverged from each other.

Our simple model demonstrates that vocal cues alone can mediate the spatial organization of primate groups. Although mechanistic information about individuals' responses to vocal communication is difficult to obtain, the non-local quality of our model allows us to use the larger- and slower-scale observations that behaviorists commonly collect to construct a reasonable characterization of the biological system. As more data become available, of course, we can revise our model to reflect new findings. As a first step, however, this simple, non-local model yields helpful qualitative results that are relevant to the types of information readily available in the field.

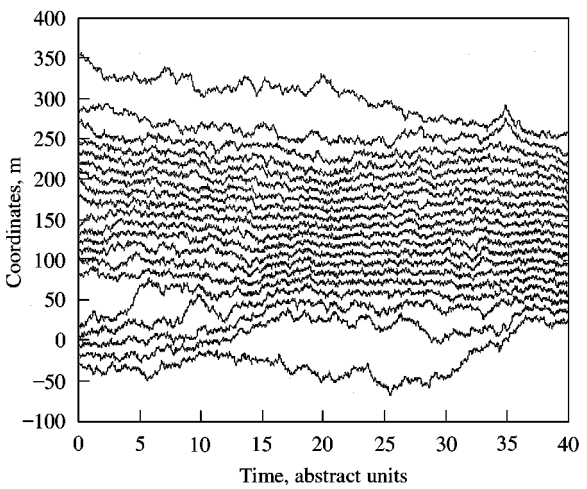

FIG. 3. Sample run of the stochastic, non-local, individual-based model of primate aggregation. From an initially random uniform distribution of 20 animals over a 400 m region, an aggregation forms so that the average distance between the neighbors in the group becomes about 10 m. Curves represent trajectories of each individual. Animals that are initially far from the group converge to the rest of the troop, while initially crowded subgroups diverge. Time units are not specified in the model.

The two examples we have presented in this section demonstrate that non-local models, by focusing on the larger and slower scales that are often of interest in biological systems, lend themselves more naturally to empirical observations than do local models that specify small-scale detail. Since a major goal of modeling biological systems is to interpret available data and make testable predictions, non-local models represent a promising approach to understanding complex phenomena.

4. Discussion

The types of models we discuss in this paper have a rich history in theoretical biology. Turing's (1952) seminal paper on the role of diffusion in pattern formation introduced spatially explicit models to biology. In the early 1970s, researchers added continuous, deterministic, directed motion to random diffusive motion in the framework of chemotaxis models (Keller & Segel, 1970). These advection–diffusion models immediately found application in ecology (see reviews in Levin & Segel, 1985; Holmes *et al.*, 1994). The familiar continuous description of diffusion can be considered a limit of the random walk, where individuals take random steps between nearest-neighboring points. Thus, diffusion and advection–diffusion equations are local in a mathematical as well as a mechanistic sense.

The next step in modeling longer-distance interactions is to allow movement between next-nearest-neighboring points. Mathematically, this kind of movement results in higher-derivative terms in the continuous description. Cohen & Murray (1981) took this initial step away from local models of continuum transport by

generalizing diffusion terms with a fourth-order spatial derivative. This "semi-local" approximation successfully explained some long-range phenomena that are impossible to represent in a local model, including pattern formation in mechanochemical systems (Murray, 1989), for example. However, the semi-local approximation eliminates certain non-local effects (Grunbaum & Okubo, 1994). For example, semi-local approximations cannot account for abrupt changes in individual density as can non-local models (Mogilner & Edelstein-Keshet, 1999).

The first truly long-range transport effects appeared in mathematical ecology in the early 1980s, most notably in Nagai & Mimura (1983). As in later work (Lewis, 1994; Mogilner & Edelstein-Keshet, 1999), early papers considered the rate of organims' advection to be a non-local function, weighted by an integral kernel, of the density of organisms. Integrals over a spatial domain where, in the integrand, a model-dependent variable is weighted by a kernel, is the main formal mathematical indicator of the non-local character of such models. Using a similar technique, Turchin (1986) obtained a more satisfactory description of insect dispersal by making its diffusion coefficient a non-local weighted function of density. In all these cases, poorly understood and presumably fast processes of information exchange between individuals underlie the structure of the integral kernels. Similar models are very popular in neurobiology (Ermentrout & Cowan, 1979), where the local dynamics of membrane potential governed by neuron-generated spikes reduce to distance-dependent strengths of recurrent excitatory connections between neurons.

In ecology and epidemiology, a different type of non-local model accomodates non-simultaneous reaction and transport for organisms that breed and disperse in different seasons (Hardin *et al*., 1988; Kot & Schaffer, 1986; Kot *et al*., 1996; Van Kirk & Lewis, 1997). These models have a form similar to eqn (4), which implicitly depends on the assumption that dispersal occurs on a much faster temporal scale than does population growth. The non-local coupling implies that the reduction of the dispersion of individuals to a spatial distribution of organisms and, therefore, to a dispersal kernel, is possible. Neubert *et al*. (1995) show elegant derivations of some of these kernels from reaction–diffusion equations.

In this paper, we restricted ourselves to analyses of interactions in real, physical space. Researchers have applied very similar ideas and mathematical techniques to the description of non-local effects in angular space (Geigant *et al*., 1998) and abstract "aspect" space such as dominance space (Jäger & Segel, 1992), shape space (Segel & Perelson, 1988), group size space (Gueron & Levin, 1995) and age space (Metz & Diekmann, 1986). In all these models unknown fast local processes, such as, for example, information exchange between bumble bees (Jager & Segel, 1992) or the action of a host of alignment-mediating proteins (Geigant *et al*., 1998), underlie non-local effects.

In conclusion, we have shown that non-local models are simplifications of complex processes that are fundamentally local. Non-local simplification is valid given a sufficient separation of scales between important processes. Although less detailed than local models, non-local models are valuable because they focus attention on the variable of primary biological interest. Even when underlying local processes are well understood, as in the chemotaxis and cellular examples in this paper, a non-local approximation may provide important insight, such as an intuitive description of distance dependence in the drift rates of individuals.

When our understanding of underlying local mechanisms is not complete, non-local models are particularly useful. They provide phenomenological descriptions of these mechanisms that may be adequate on the scale of the variable of interest. Similarly, gathering data on spatial pattern is often easier than gathering data on the processes underlying the pattern. Consequently, biological data for spatial systems are often insufficient to parameterize or test a mechanistic local model but are suitable for a reduced non-local model.

A further advantage of non-local models is that they can accommodate discreteness in a biological system far more easily than can local models. For instance, when the number of individuals to be modeled is small, local models written in terms of density functions become very awkward. On the other hand, non-local models can be

written in terms of individuals' coordinates, thereby accommodating discrete individuals. In particular, Durrett & Levin (1994) have shown that non-local discrete models may exhibit fundamentally different dynamics from local models, in essence because of a separation of scales.

In addition to their suitability for biological situations, non-local models are often no more difficult to analyse than are local models. Linear stability analysis (Levin & Segel, 1985), numerical analysis (Bellomo & Preziosi, 1995) and singular perturbation theory (Mogilner *et al*., 1996) are equally applicable to both local and non-local models. The extra cost of evaluating integrals at each iteration in the non-local models is alleviated by the fact that non-local approximations effectively eliminate processes occurring at fast temporal scales. Therefore, one may choose large steps of numerical integration, vastly reducing the computational expense of the integro-PDE. In all, we conclude that non-local modeling is a powerful technique that can greatly facilitate continuing efforts to use mathematics to understand biology.

This paper is a result of a research and training project of a multidisciplinary group concerned with understanding the role of non-locality in nonlinear biological dynamics. The corresponding activities were made possible by the support from RTG NSF Grant DBI-9602226 "Nonlinear dynamics in biology". The grant is administered through the Institute for Theoretical Dynamics at the University of California at Davis. We are grateful for long and fruitful discussions with M. Lewis, M. Kot, B. Ermentrout and E. Holmes that helped us to formulate the ideas of the present work. We also thank A. Amezcua and G. Takimoto for their help at early stages of this project.

The co-PIs for this grant, A. Hastings, J. Keizer, A. Cheer and M. Stanton, provided us with constant inspiration and support. We particularly wish to acknowledge Joel Keizer, whose insight, critical thinking, and frank kindness were invaluable to us as individuals and as a group. We dedicate this paper to his memory, and we hope that this and future work meet the high standards that he set for us by his example.

REFERENCES

ALT, W. (1980). Biased random walk models for chemotaxis and related diffusion approximation. *J. Math. Biol.* **9,** 147–177.

ANDOW, D. A., KAREIVA, P. M., LEVIN, S. A. & OKUBO, A. (1990). Spread of invading organisms. *Landscape Ecol.* **4,** 177–188.

BELLOMO, N. & PREZIOSI, L. (1995). *Modelling Mathematical Methods and Scientific Computations*. Boca Raton, FL: CRC Press.

BRAY, D. (1992). *Cell Movements*. New York: Garland.

CHILDRESS, S. & PERCUS, J. K. (1981). Nonlinear aspects of chemotaxis. *Math. Biosci.* **56,** 217–237.

COHEN, A. H. & MURRAY, J. D. (1981). A generalized diffusion model for growth and dispersal in a population. *J. Math. Biol.* **12,** 237–249.

DURRETT, R. & LEVIN, S. A. (1994). The importance of being discrete and spatial. *Theor. Popul. Biol.* **46,** 363–394.

DWORKIN, M. & KAISER, D. (1985). Cell interactions in myxobacterial growth and development. *Science* **230,** 18–24.

EDELSTEIN-KESHET, L. & ERMENTROUT, G. B. (1990). Models for contact mediated pattern formation. *J. Math. Biol.* **29,** 33–58.

ERMENTROUT, G. B. & COWAN, J. D. (1979). A mathematical theory of visual hallucination patterns. *Biol. Cybernet.* **34,** 137–150.

FISHER, R. A. (1937). The wave of abundance of advantageous genes. *Ann. Eugenics* **7,** 335–369.

GARCIA, A. L. (1994). *Numerical Methods for Physics*. Englewood Cliffs, NJ: Prentice-Hall.

GAUTIER, J.-P. & GAUTIER, A. (1977). Communication in Old World monkeys. In: *How Animals Communicate* (Sebeok, T., ed.), pp. 890–964. Bloomington: Indiana University Press.

GEIGANT, E., LADIZHANSKY, K. & MOGILNER, A. (1998). Integro-differential model for orientational distribution of polymers in cells. *SIAM J. Appl. Math.* **59,** 787–809.

GRINDROD, P. (1988). Models of individual aggregation or clustering in single and multi-species communities. *J. Math. Biol.* **26,** 651–660.

GRINDROD, P., MURRAY, J. D. & SINHA, S. (1989). Steady-state spatial patterns in a cell-chemotaxis model. *IMA J. Math. Appl. Med. Biol.* **6,** 69–79.

GRUNBAUM, D. & OKUBO, A. (1994). Modelling social animal aggregation. In: *Frontiers in Mathematical Biology* (Levin, S., ed.), pp. 296–325. New York: Springer.

GUERON, S. & LEVIN, S. A. (1995). The dynamics of group formation. *Math. Biosci.* **128,** 243–264.

HARDIN, D. P., TAKAC, P. & WEBB, G. F. (1988). A comparison of dispersal strategies for survival of spatially heterogeneous populations. *SIAM J. Appl. Math.* **48,** 1396–1423.

HOLMES, E. E., LEWIS, M. A., BANKS, J. E. & VEIT, R. R. (1994). PDE in ecology: spatial interactions and population dynamics. *Ecology* **75,** 17–29.

JÄGER, E. & SEGEL, L. A. (1992). On the distribution of dominance in populations of social organisms. *SIAM J. Appl. Math.* **52,** 1444–1468.

KELLER, E. F. & SEGEL, L. A. (1970). Initiation of slime mold aggregation viewed as an instability. *J. theor. Biol.* **26,** 399–415.

KIERSTEAD, H. & SLOBODKIN, L. B. (1953). The size of water masses containing plankton bloom. *J. Marine Res.* **12,** 141–147.

KOT, M., LEWIS, M. A. & VAN DEN DRIESSCHE, P. (1996). Dispersal data and the spread of invading organisms. *Ecology* **77,** 2027–2042.

KOT, M. & SCHAFFER, W. M. (1996). Discrete-time growth-dispersal models. *Math. Biosci.* **80,** 109–136.

LEVIN, S. A. (1992). The problem of pattern and scale in ecology. *Ecology* **73,** 1943–1967.

LEVIN, S. A. & SEGEL, L. A. (1985). Pattern generation in space and aspect. *SIAM Rev.* **27,** 45–67.

LEWIS, M. A. (1994). Spatial coupling of plant and herbivore dynamics—the contribution of herbivore dispersal to transient and persistent waves of damage. *Theor. Popul. Biol.* **45,** 277–312.

LIN, C. C. & SEGEL, L. A. (1974). *Mathematics Applied to Deterministic Problems in the Natural Sciences.* New York: Macmillan.

LINDBURG, D. G. (1971). The rhesus monkey in North India: an ecological and behavioral study. In: *Primate Behavior* (Rosenblum, L. A., ed.), pp. 1–106. New York: Academic Press.

MACKAS, D. L. & BOYD, C. M. (1979). Spectral analysis of zooplankton spatial heterogeneity. *Science* **204,** 62–64.

METZ, J. A. J. & DIEKMANN, O. (1986). *The Dynamics of Physiologically Structured Populations*, Berlin: Springer.

MIMURA, M., TSUJIKAWA, T., KOBAYASHI, R. & UEYAMA, D. (1993). Dynamics of aggregating patterns in a chemotaxis–diffusion–growth model equation. *Forma* **8,** 179–195.

MITCHISON, G. (1980). A model for vein formation in higher plants. *Proc. R. Soc. London B* **207,** 79–109.

MOGILNER, A. & EDELSTEIN-KESHET, L. (1999). A non-local model for a swarm. *J. Math. Biol.* **38,** 534–570.

MOGILNER, A., EDELSTEIN-KESHET, L. & ERMENTROUT, G. B. (1996). Selecting a common direction. II. Peak-like solutions representing total alignment of cell clusters. *J. Math. Biol.* **34,** 811–842.

MOLLISON, D. (1977). Spatial contact models for ecological and epidemic spread. *J. R. Stat. Soc. Ser. B* **39,** 283–326.

MORSE, P. M. & FESHBACH, H. (1953). *Methods of Theoretical Physics.* New York: McGraw-Hill.

MURRAY, J. D. (1981). A prepattern formation mechanism for animal coat markings. *J. theor. Biol.* **88,** 161–199.

MURRAY, J. D. (1989). *Mathematical Biology*. New York: Springer-Verlag.

MURRAY, J. D., OSTER, G. F. & HARRIS, A. K. (1983). A mechanical model for mesynchymal morphogenesis. *J. Math. Biol.* **17,** 125–129.

NAGAI, T. & MIMURA, M. (1983). Asymptotic behaviour for a nonlinear degenerate diffusion equation in population dynamics. *SIAM J. Appl. Math.* **43,** 449–464.

NANJUNDIAH, V. (1973). Chemotaxis, signal relaying and aggregation morphology. *J. theor. Biol.* **42,** 63–105.

NEUBERT, M. G., KOT, M. & LEWIS, M. A. (1995). Dispersal and pattern formation in a discrete-time predator–prey model. *Theor. Popul. Biol.* **48,** 7–43.

ODELL, G., OSTER, G., ALBERCH, P. & BURNSIDE, B. (1981). The mechanical basis of morphogenesis. I. Epithelial folding and invagination. *Dev. Biol.* **85,** 446–462.

OKUBO, A. (1980). *Diffusion and Ecological Problems*: *Mathematical Models.* Berlin: Springer.

OSTER, G. & MURRAY, J. D. (1989). Pattern formation models and developmental constraints. *J. Exp. Zool.* **251,** 186–202.

OTHMER, H. G., DUNBAR, S. R. & ALT, W. (1988). Models of dispersal in biological systems. *J. Math. Biol.* **26,** 263–298.

OTHMER, H. G. & STEVENS, A. (1997). Aggregation, blowup and collapse: the ABC's of generalized taxis. *SIAM J. Appl. Math.* **57,** 1044–1081.

PALOMBIT, R. A. (1992). A preliminary study of vocal communication in wild long-tailed macaques (*Macaca fascicularis*). II. Potential of calls to regulate intragroup spacing. *Int. J. Primatol.* **13,** 183–207.

PETTERSSON, J. (1993). Odour stimuli affecting autumn migration of *Rhopalosiphum padi*. *Ann. Appl. Biol.* **122,** 417–425.

ROBINSON, J. G. (1982). Vocal systems regulating within-group spacing. In: *Primate Communication* (Snowdon, C. T., Brown, C. H. & Petersen, M. R., eds), pp. 94–116. Cambridge: Cambridge University Press.

RODIONOV, V. I. & BORISY, G. B. (1997). Self-centring activity of the cytoplasm. *Nature* **386,** 170–173.

SEGEL, L. A. & PERELSON, A. S. (1988). Computations in shape space: an approach to network theory. In: *Theoretical Immunology II* (Perelson, A. S., ed.), pp. 321–343. Reading, MA: Addison–Wesley.

SHI, W. & ZUSMAN, D. R. (1994). Sensory adaptation during negative chemotaxis in *Myxococcus xanthus*. *J. Bacteriol.* **176,** 1517–1520.

SKELLAM, J. G. (1951). Random dispersal in theoretical populations. *Biometrica* **38,** 196–218.

SPORMANN, A. M., & KAISER, D. (1995). Gliding movements in *Myxococcus xanthus*. *J. Bacteriol.* **177,** 5846–5852.

STEELE, J. H. (1974). *The Structure of Marine Ecosystems.* Cambridge, MA: Harvard University Press.

STEELE, J. H. (1976). Patchiness. In: *The Ecology of the Sea* (Cushing, D. H. & Walsh, J. H., eds), pp. 98–115. Philadelphia: Saunders.

STEELE, J. H. (1978). *Spatial Pattern in Plankton Communities.* New York: Plenum Press.

TURCHIN, P. (1986). Models for aggregating populations. In: *Mathematical Ecology* (Hallam, T. G., ed.), pp. 101–127. Singapore: World Scientific.

TURCHIN, P. & KAREIVA, P. (1989). Aggregation in *Aphis varians*: an effective strategy for reducing predation risk. *Ecology* **70,** 1008–1061.

TURING, A. M. (1952). The chemical basis of morphogenesis. *New Phytol.* **54,** 39–48.

VAN KIRK, R. W. & LEWIS, M. A. (1997). Integrodifference models for persistence in fragmented habitats. *Bull. Math. Biol.* **59,** 107–137.

WARBURTON, K. & LAZARUS, J. (1991). Tendency-distance models of social cohesion in animal groups. *J. theor. Biol.* **150,** 473–488.

WAY, M. & CAMMELL, M. (1970). Aggregation behavior in relation to food utilization in aphids. In: *Animal Populations in Relation to Their Food Resources* (Watson, A., ed.), pp. 229–247. London: Blackwell Scientific Publications.

WEAST, R. C., ASTLE, M. J. & BEYE, W. H. (1983). *CRC Handbook of Chemistry and Physics.* Boca Raton, FL: CRC Press.